Tailoring The Vibrational Infrared And Raman Spectra Of Samarium Oxide Doped Magnesium Tellurite Glass Containing Silver Nanoparticles

Nurulhuda Mohammad Yusoff, Md Rahim Sahar, Siti Maisarah Aziz, Salmiah Jamal Mat Rosid, Siti Noor Syuhada

Abstract: The material under investigation was tellurite glass based composition of (89.6-x)TeO_2-10MgO-(x)Sm_2O_3-0.4AgCl with $0.2 \leqslant x \leqslant 1.2$ mol% glass system. The glass samples have been synthesised by a conventional melt quenching technique. The amorphous nature has been verified by X-ray diffraction pattern. The effect of samarium doping on the structural properties of glass system was performed by FTIR and Raman spectroscopy. Analysis of FTIR and Raman spectroscopy indicated the presence of three main bands attributed to the structural units, [TeO_4] tbp, [TeO_{3+1}] polyhedral, and [TeO_3] tp. The substitution of samarium ion, Sm^{3+} at different concentration in the glass structure led to the appearance of overlapping band and shifting of wavenumber. This demonstrated that, Sm^{3+} significantly transformed [TeO_4] tbp to [TeO_3] tp through [TeO_{3+1}] polyhedral. The structural change was discussed in terms of formation of bridging oxygen (BO) and non-bridging oxygen (NBO) with respect to glass composition. The formation of NBO was responsible to decrease the connectivity of the tellurite glass former network.

Index Terms : Glass, Samarium, Fourier Transform Infrared Spectroscopy, Raman Spectroscopy

1 INTRODUCTION

In the field of oxide glasses discovery, great importance has been focused on structural modification as a part to achieve enhancement in optical and even more so in having laser feature, in addition to forming strong glass structure. According to tellurium oxide glass nature, transition metal is required in order to form stable glass with promising properties such as absence of hygroscopic, high chemical durability, high refractive index, high density, strong linear and non-linear response [1]. More importantly, tellurium matrix glass is a wonderful host for rare earth doping activity which provides minimum radiation loses - simply said that is a low phonon energy for rare earth dopant. Many glass researchers discussed rare earth in the build of luminescence feature in term of energy transfer [2], up-conversion luminescence due to potential in converting light [3-5] instead of structure modification function. Rare earth ions naturally participate in overall glass bonding to tailor the desired properties since their structural roles in the glass structure are related to their size and coordination number [6]. The fact is, introduction of rare earth ion increases nonbridging anions which affects the discontinuity of glass network [6]. Clearly, the properties of oxide glasses are strongly dependent on the nature and the concentration of the constituent oxides, which makes the investigation of structural properties being the important subject to be studied. This work presented structural study through Infrared and Raman spectra. We focused on evaluating the possibility modification of structural units according to substitution of different concentration of Sm_2O_3 into glass matrix. The promising and stable compositions (89.6-x)TeO_2-10MgO-(x)Sm_2O_3-0.4AgCl with $0.2 \leq x \leq 1.2$ mol% was investigated. Special attention was paid to the complement between FTIR and Raman resulted in detecting the change of short range order glass structure with respect to the formation of bridging or non-bridging oxygen.

2 METHODOLOGY

2.1 Sample Preparation

Glass samples were prepared by using melt quenching technique. The raw materials were in powder form with high grade purity chemicals (99.9%) of Tellurium oxide (TeO_2), Magnesium oxide (MgO), Samarium oxide (Sm_2O_3) and Silver chloride (AgCl). The required proportion of TeO_2, MgO, Sm_2O_3 and AgCl powder based on the nominal compositions (89.6-x)TeO_2-10MgO-(x)Sm_2O_3-0.4AgCl with $0.2 \leq x \leq 1.2$ mol% were weighted using high precision balance (Electronic Balance Precise 205A SCS ±0.001g). The total weight of each batch of glass was 15 gram. Table 1 shows the nominal composition of glass system.

- *Nurulhuda Mohammad Yusoff is currently a senior lecturer at UniSZA Science and Medicine Foundation Centre, Universiti Sultan Zainal Abidin, Gong Badak,vTerengganu, Malaysia. Email: nurulhudamy@unisza.edu.my*
- *Md. Rahim Sahar is currently Professor at Faculty of Science, Universiti Teknologi Malaysia, Skudai, Johor, Malaysia.*
- *Siti Maisarah Aziz is a senior lecturer at UniSZA Science and Medicine Foundation Centre, Universiti Sultan Zainal Abidin, Gong Badak,vTerengganu, Malaysia.*
- *Salmiah Jamal Mat Rosid is a senior lecturer at UniSZA Science and Medicine Foundation Centre, Universiti Sultan Zainal Abidin, Gong Badak,vTerengganu, Malaysia.*
- *Siti Noor Syuhada Mohd @ Muhammad Amin is a lecturer at UniSZA Science and Medicine Foundation Centre, Universiti Sultan Zainal Abidin, Gong Badak, Terengganu, Malaysia.*

TABLE 1
NOMINAL COMPOSITION OF GLASS SYSTEM (IN MOL%)

Sample code	TeO_2	MgO	Sm_2O_3	AgCl
S1	89.4	10.0	0.2	0.4
S2	89.2	10.0	0.4	0.4
S3	88.8	10.0	0.8	0.4
S4	88.6	10.0	1.0	0.4
S5	88.4	10.0	1.2	0.4

The weighed powder was mixed together using milling machine for about 30 minutes to make sure the starting mixture was homogenous before melting process. The mixture was then transformed into platinum crucible for being placed in high temperature electrical furnace at 900 - 950 °C for 45 min. The molten liquid was shaken frequently and vigorously to ensure proper melt would be bubble free. The melt was poured into a brass mould that was placed in annealing surface after the desired viscosity was achieved. The samples were kept in annealing process for 3 h at 300 °C to remove the thermal and mechanical strains completely. Afterward, the furnace was switched off and the samples were then cooled down to room temperature. The prepared sample was stored in vacuumed desiccators to assure dry and humidity-free storage. Prepared glasses were cut into small pieces and crushed into powder form for X-Ray and structural characterisations.

2.2 X-Ray Diffraction

X-Ray Diffraction measurement was performed using powdered glass samples on high resolution X-ray diffractometer system model of PANalytical X'Pert PRO MRD PW3040 with Cu Kα radiation (λ = 1.54Å) in the 2θ range of 10°–80° at a step scan time of 2.5 seconds. The X-ray tube was operated at running voltage 40 kV and current 35 mA. The scattered X-ray intensity was measured with a scintillation detector.

2.3 Fourier Transform Infrared (FTIR)

Infrared spectrum of glass sample was recorded by Perkin Elmer Fourier Transform Infrared (FTIR) spectrometer using KBr disk technique in the wavenumber ranging from 4000 cm^{-1} to 400 cm^{-1} at room temperature. The mixture of 0.02 mg powdered glass sample and 2 mg spectroscopic grade KBr were mixed and ground in agate mortar. The mixture was subjected to pressure of 10 tons using hydraulic press machine for 5 minutes in order to prepare thin pellets with surface area of 1 cm^2. The FTIR absorption spectra were measured immediately after preparing the pellets.

2.4 Raman Spectroscopy

Raman scattering studies were performed on glass samples with Jobin Yvon HR 800 UV Raman spectrometer using argon ion laser (20mW) as excitation source. Powdered sample of about 10 mg was inserted into a sample holder made of alumina. Measurements were carried out at room temperature in the backscattering geometry, in the wave number ranging from 100 to 1200 cm^{-1}.

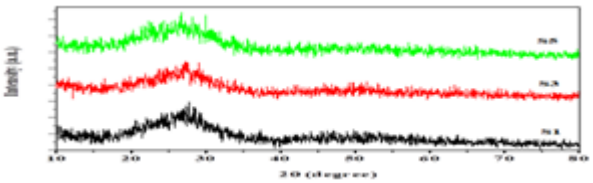

Fig. 1. Typical X-ray diffraction patterns of (89.6-x) TeO_2-10MgO-xSm_2O_3-0.4AgCl glass system

3 Results and Discussion

The XRD pattern of the prepared glass has been recorded in the range of 10° to 80°as displayed in Fig. 1. The samples were almost completely amorphous since no sharp peak was observed, indicating the absence of regular three-dimensional molecular lattice structure, typical of crystalline materials [7-9]. It was observed that only representative broad peak at lower angles ranging from 20° to 40°, which is the characteristic of short-range order, confirmed the amorphous nature of tellurite glass [10-11]. The tellurite glasses consisted of two main IR absorption bands, one was due to tetrahedral TeO_4 units and the other was due to the trigonal TeO_3 units, which confirmed the characteristic of tellurite glass [12-13]. The obtained IR spectra of all investigated glass samples showed quite similar band shapes and are presented in Fig. 2 in the spectral ranging from 450-4000 cm^{-1}. All the absorption peaks are listed in Table 2 and the result were comparable to other tellurite glass systems [12, 14-18]. From Table 2, it shows that the addition of Sm_2O_3 from 0.2 to 0.8 mol% provided the formation of [TeO_{3+1}] polyhedral which represented by the band overlapping of [TeO_4] tbp and [TeO_3] tp groups which was located in the range of 719 – 739 cm^{-1}. However, at 1.0 mol% Sm_2O_3, the overlapping band split up into two strong bands located at 663 and 772 cm^{-1} with respect to [TeO_4] tbp and [TeO_3] tp. This indicated the formation of bridging oxygen was connected to TeO_4 and non-bridging oxygen were connected to TeO_3. Further addition of Sm_2O_3 up to 1.2 mol% again showed the overlapping of [TeO_4] tbp and [TeO_3] tp bands at 727 cm^{-1} which indicated that the formation of NBO in term of $Te\text{-}O^-$ bond was connected to TeO_{3+1} polyhedral. The occurrence band in the range of 1630 – 1656 cm^{-1} and 3308 – 3369 cm^{-1} were corresponding to H-O-H
bending and OH stretching vibration, respectively.

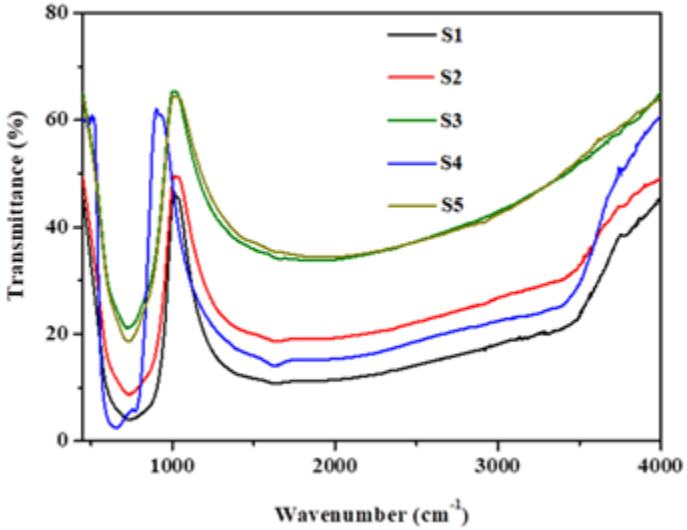

Fig. 2. IR spectra of (89.6-x)TeO_2-10MgO-xSm_2O_3-0.4AgCl glass system

TABLE 2
IR ABSORPTION PEAK (IN CM^{-1}) OF MAGNESIUM TELLURITE GLASS SYSTEM

Sample Code	Te-O-Te or O-Te-O bond	[TeO_4] tbp	[TeO_{3+1}] Polyhedra	[TeO_3] tp	H-O-H bending	OH stretching
S1	disappear	disappear	739	disappear	1636	3308
S2	disappear	disappear	738	disappear	1639	3354
S3	disappear	disappear	719	disappear	1656	3369
S4	504	663	disappear	772	1632	3353
S5	disappear	disappear	727	disappear	1630	3310

Fig. 3 shows the Raman spectra of glass system. Since the inelastic energy range of Raman scattering was relatively lower than that of vibrational energy, the wavenumber range was taken from 100-1200 cm^{-1}, which was slightly lower in the IR spectral range. This was the most suitable range to get the best Raman intensity. The Raman spectra were discussed based on wavenumber shift and intensity. The assignments of Raman band positions are summarised in Table 3. It is noted out that the result for S4 is taken from previous published paper (labelled as S3) [19]. From Table 3, it can be seen that the Raman spectra could be divided into two wavenumber regions: higher wavenumber around 400 - 1200 cm^{-1} and the universal Raman band, which normally present in non-crystalline solids including glasses centred at lower wavenumber (<200 cm^{-1}) also known as Boson peak (BP) [20-21]. The observed Raman bands comparable to various tellurite glasses as discussed and reported in Table 4.

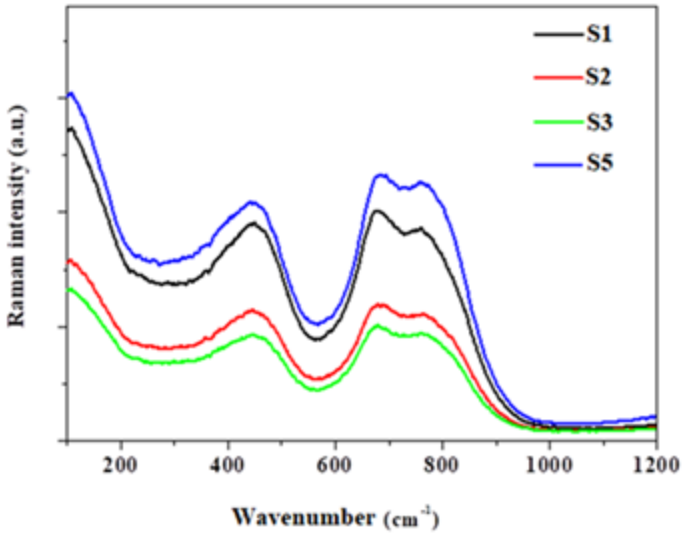

Fig. 3. Raman spectra of (89.6-x)TeO_2-10MgO-xSm_2O_3-0.4AgCl glass system

TABLE 3
RAMAN BAND ASSIGNMENT (IN CM^{-1}) OF MAGNESIUM TELLURITE GLASS SYSTEM

Sample Code	Boson peak, BP	Symmetrical stretching or bending Te-O-Te or O-Te-O linkages	$(Te_{ax}\text{-}O)_3$ of [TeO_4] tbp units	$(Te_{ax}\text{-}O)_3$ and $(Te_{eq}\text{-}O)_3$ vibrational modes of [TeO_{3+1}] polyhedral	[TeO_3] tp group
S1	disappear	449	679	759	771
S2	disappear	445	679	762	770
S3	disappear	448	680	760	772
S4	151	425	646	720	770
S5	disappear	443	695	756	774

TABLE 4
RAMAN BAND ASSIGNMENT (IN CM^{-1}) OF VARIOUS TELLURITE GLASS SYSTEMS

Glass system	Boson peak (cm^{-1})	Symmetrical stretching or bonding Te-O-Te linkage (cm^{-1})	TeO_4 tbp (cm^{-1})	TeO_{3+1} polyhedral /TeO_3 tp (cm^{-1})	Ref.
Sm^{3+} doped niobium borotellurite glass	83	460	Not reported	Not reported	[22]
TeO_2–ZnO-Na_2O-WO_3-Er_2O_3-Ce_2O_3	Not reported	450	660	765	[23]
TeO_2–ZnO–CdO–Li_2O–V_2O_5	-	408	665	748	[24]
TeO_2–TiO_2–Nd_2O_3-WO_3	115	445	660	740	[20]
TeO_2–ZnO–Na_2O–WO_3–Er_2O_3–Tm_2O_3	130	450	675	765	[25]
TeO_2-PbO	120	~ 450	~ 600	~ 700	[26]

From Fig. 3, it can be seen that the strongest sharp peak observed was ranging from 646 – 695 cm^{-1}. Fig. 4 shows the variation of TeO_4 tbp and TeO_3 tp peak wavenumber versus Sm_2O_3 concentration. It was observed that the addition of Sm_2O_3 from 0.2 to 0.4 mol% showed that the TeO_4 peak remained at the same wavenumber and only slightly shifted to higher wavenumber when the concentration of Sm_2O_3 was up to 0.8 mol%. This indicated that the formation of non-bridging oxygen remained the same. However, there was an obvious decreasing in wavenumber of TeO_4 band as the addition of Sm_2O_3 was up to 1.0 mol%. This reflected to the formation of bridging oxygen instead of non-bridging oxygen in the glass matrix and this result was in parallel with the IR spectra as shown in Fig. 2. Further increasing of Sm_2O_3 concentration up to 1.2 mol% showed that the wavenumber was increased toward higher wavenumber. At this point, it was believed that the glass matrix contained the intermediate state of [TeO_{3+1}] polyhedral and [TeO_3] tp with non-bridging oxygens which led the shifting toward higher wavenumber. However, in IR spectra, there was undetectable of [TeO_3] tp at 1.2 mol% Sm_2O_3. The actual band position of [TeO_{3+1}] polyhedral and [TeO_3] tp presented around 720 – 762 cm^{-1} and at shoulder around 770 – 774 cm^{-1}, respectively. The band around 425 – 449 cm^{-1} was assigned for Te-O-Te or O-Te-O linkage.

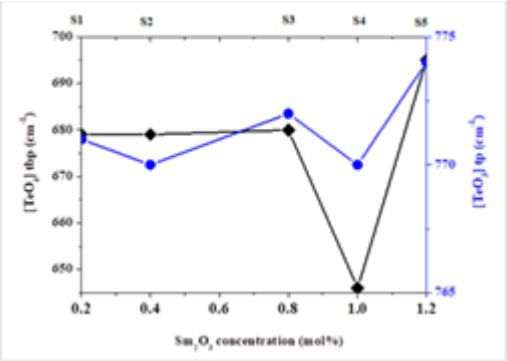

Fig. 4. The wavenumber of TeO_4 tbp and TeO_3 tp versus Sm_2O_3 concentration

4 Conclusion

From the discussions above, the following conclusions can be drawn. The glass of composition 89.6-x)TeO_2-10MgO-xSm_2O_3-0.4AgCl with 0.2 ≤ x ≤ 1.2 mol% has successfully been prepared. The XRD, FTIR and Raman spectra have been investigated in order to have deeper understanding about glass structural properties. All glasses are amorphous in nature. The alteration in structural properties was majorly attributed to the distortion of TeO_4 tetrahedra. The addition of Sm_2O_3 content led to an increase in [TeO_4] wavenumber and to the open structure of the glasses. The formation of TeO_{3+1} as shown in FTIR spectra confirmed the distortion of TeO_4 tetrahedra. This was complementrary with Raman spectra that showed the appearance of TeO_3 peak and almost shifted toward higher wavenumber.

Acknowledgement

The authors gratefully acknowledge the financial support from UTM and Malaysian Ministry of Education through the Vot. 4L032. Also, a special thanks to UTM for providing the measurement facilities.

References

[1] Azlan, M. N., Halimah, M. K., Shafinas, S. Z., & Daud, W. M. (2015). Electronic polarizability of zinc borotellurite glas system containing erbium nanoparticles. Materials Express, 5 (3), 211-218

[2] Amjad, R. J., Dousti, M.R., Sahar, M.R., Shaukat, S.F., Ghoshal, S.K., Sazali, E.S., Nawaz, F. (2014). Silver Nanoparticles enhanced luminescence of Eu3+ doped Tellurite Glass, Journal of Luminescence 154 (2014) 316 – 321.

[3] Aisaka, T., Fujii, M., Hayashi, S. (2008). Enhancement of Upconversion luminescence of Er doped Al_2O_3 films by Ag Island films, Appl.Phys. Lett. 92 132105.

[4] Yi, G. S., Zhao, S. Y., Ge, Y., Yang, W. J., Chen, D. P., Guo, L. H. (2004). Synthesis, Characterization, and Biological Application of Size-Controlled Nanocrystalline NaYF4:Yb, Er Infrared-to-visible Up-Conversion Phosphors. Nano Letters 4 (11) 2191-2196.

[5] Wang, L. Y., Yan, R. X., Li, Y. D., (2005). Fluorescence Resonant Energy Transfer Biosensor Based on Upconversion Luminescent Nanoparticles. Angew Chem. Int. Ed. 44 6054.

[6] Ohashi, M., Nakamura, K., Hirao, K., Kanzaki, S., Hampshire, S. (1995). Formation and properties of Ln–Si–O–N Glasses (Ln 1⁄4 Lanthanides or Y), J. Am. Ceram. Soc. 78: 71–76.

[7] Wu, L. Zhou, Y., Zhou, Z., Cheng, P., Huang, B., Yang, F., Li, J. (2016). Effect of silver nanoparticles on the 1.53 mm fluorescence in Er3+/Yb3+ codoped tellurite glasses, Opt. Mater. 57 : 185e192.

[8] Soltani, I., Hraiech, S., Horchani-Naifer, K., Massera, J., Petit, L., Ferid, M. (2016). Thermal, structural and optical properties of Er3+ doped phosphate glasses containing silver nanoparticles, J. Non-Cryst. Solids 438: 67e73

[9] Jayasimhadri, M., Cho, E.-J., Jang, K.-W., Lee, H.S., Kim, S.I., (2008). Spectroscopic properties and Judd-Ofelt analysis of Sm3+ doped lead germinate tellurite glasses, J. Phys. Appl. Phys. 41: 175101.

[10] Nazrin, S.N., Halimah, M.K., Muhammad, F.D., Yip, J.S., Hasnimulyati, L., Faznny, M. F., Hazlin, M. A., Zaitizila, I., (2018). The effect of erbium oxide in physical and structural properties of zinc tellurite glass system. Journal of Non-Crystalline Solids 490 : 35–43.

[11] Zhu, Y., Shen, X., Su, X., Zhou, M., Zhou, Y., Li, J., Yang, G., (2019). Concentration dependent structural, thermal and luminescence properties in Er3+/Tm3+ doped tellurite glasses. Journal of Non-Crystalline Solids 507 : 19–29.

[12] Rada, S., Culea, M., Culea, E. (2008). Structure of TeO_2 -B_2O_3 Glasses Inferred from Infrared Spectroscopy and DFT Calculations. Journal of Non-Crystalline Solids. 354: 5491-5495.

[13] Simon, I. Modern Aspects of the Vitreous state. London: Butterworth. 1964.

[14] Dousti, M.R., Sahar, M.R., Ghoshal, S.K., Amjad, R.J., Samavati, A.R. (2013). Effect of AgCl on Spectroscopic Properties of Erbium doped Zinc Tellurite Glass. Journal of Molecular Structure. 1035: 6 -12

[15] Leng, Y. Materials Characterization: Introduction to Microscopic and Spectroscopic Methods. New Jersey: John Wiley & Sons. 2008.

[16] Awang, A., Ghoshal, S.K., Sahar, M.R., Arifin, R. (2015). Gold Nanoparticles Assisted Structural and Spectroscopic Modification in Er^{3+}, Optical Materials. 42: 495-505.

[17] Rada, S., Dan, V., Rada, M., Culea, E. (2010). GadoliniumEnvironment in Borate–Tellurate Glass Ceramics Studied by FTIR and EPR Spectroscopy. Journal of Non-Crystalline Solids. 356: 474-479.

[18] Gowda, V. C. V., Reddy, C. N., Radha, K. C., Anavekar, R. V., Etourneou, J., Rao, K. J. (2007). Structural Investigations of Sodium Diborate Glasses Containing PbO, Bi_2O_3 and TeO_2: Elastic Property Measurements and Spectroscopic Studies. Journal of Non-Crystalline Solids. 353: 1150-1163.

[19] Yusoff, N. M., Sahar, M. R. (2015). The incorporation of silver nanoparticles in samarium doped magne- sium tellurite glass: Effect on the characteristic of bonding and local structure, PhysicaB470-471(2015)6–14.

[20] Fares, H., Jlassi, I., Elhouichet, H., Férid, M. (2014). Investigations of Thermal, Structural and Optical

Properties of Tellurite Glass with WO_3 adding. Journal of Non-Crystalline Solids. 396–397: 1–7.

[21] Suthanthirakumar, P., Karthikeyan, P., Manimozhi, P.K., Marimuthu, K. (2015). Structural and Spectroscopic Behavior of Er^{3+}/Yb^{3+} co-doped Boro-tellurite Glasses. Journal of Non-Crystalline Solids. 410: 26-34.

[22] Ravi, O., Reddy, C. M., Manoj, L. and Raju, B. D. P. (2012). Structural and Optical Studies of Sm^{3+} ions doped Niobium Borotellurite Glasses. Journal of Molecular Structure. 1029: 53-59.

[23] Zheng, S., Zhou, Y., Yin, D., Xu, X., Wang, X. (2013). Influence of WO_3 on the Spectroscopic Properties and Thermal Stability of Er^{3+}/Ce^{3+} codoped Tellurite Glasses. Optical Materials. 35: 1526-1531.

[24] Sreenivasulu, V., Upender, G., Swapna, Priya, V. V., Mouli, V. C., Prasad, M. (2014). Raman, DSC, ESR and Optical Properties of Lithium Cadmium Zinc Tellurite Glasses. Physica B. 454: 60–66.

[25] Yin, D., Qi, Y., Peng, S., Zheng, S., Chen, FF., Yang, G., Wang, X., Zhou, Y. (2014). Er^{3+}/Tm^{3+} Codoped Tellurite Glass for Blue Upconversion—Structure, Thermal Stability and Spectroscopic Properties. Journal of Luminescence.146: 141–149.

[26] Khatir, S., Romain, F., Portier, J., Rossignol, S., Tanguy, B., Videau, J. J., Turrell, S. (1993). Raman Studies of Recrystallized Glasses in the Binary, TeO_2-PbO System. Journal of Molecular Structure. 298:13.